NASA TECHNICAL MEMORANDUM

NASA TM X-73,129

NASA TM X-73,129

AN EFFICIENT NUMERICAL METHOD FOR SOLVING THE TIME-DEPENDENT COMPRESSIBLE NAVIER-STOKES EQUATIONS AT HIGH REYNOLDS NUMBER

Robert W. MacCormack

Ames Research Center
Moffett Field, Calif. 94035

(NASA-TM-X-73129) AN EFFICIENT NUMERICAL METHOD FOR SOLVING THE TIME-DEPENDENT COMPRESSIBLE NAVIER-STOKES EQUATIONS AT HIGH REYNOLDS NUMBER (NASA) 18 p HC $3.50 CSCL 20D G3/02

N76-27175

Unclas 45810

July 1976

1. Report No.	2. Government Accession No.	3. Recipient's Catalog No.
TM X-73,129		

4. Title and Subtitle	5. Report Date
AN EFFICIENT NUMERICAL METHOD FOR SOLVING THE TIME-DEPENDENT COMPRESSIBLE NAVIER-STOKES EQUATIONS AT HIGH REYNOLDS NUMBER	6. Performing Organization Code

7. Author(s)	8. Performing Organization Report No.
Robert W. MacCormack	A-6580
	10. Work Unit No. 505-06-12-07
9. Performing Organization Name and Address	11. Contract or Grant No.
Ames Research Center Moffett Field, California 94035	13. Type of Report and Period Covered
12. Sponsoring Agency Name and Address	Technical Memorandum
National Aeronautics and Space Administration Washington, D.C. 20546	14. Sponsoring Agency Code

15. Supplementary Notes

16. Abstract

This paper describes a new numerical method that has been used to drastically reduce the computation time required to solve the Navier-Stokes equations at flight Reynolds numbers. Though flows past complete aircraft configurations are still beyond our reach, the new method makes it possible and practical to calculate many important three-dimensional, high Reynolds number flow fields on today's computers.

17. Key Words (Suggested by Author(s))	18. Distribution Statement
Compressible Navier-Stokes High Reynolds number Numerical analysis	Unlimited STAR Category - 02

19. Security Classif. (of this report)	20. Security Classif. (of this page)	21. No. of Pages	22. Price*
Unclassified	Unclassified	17	$3.25

*For sale by the National Technical Information Service, Springfield, Virginia 22161

AN EFFICIENT NUMERICAL METHOD FOR SOLVING THE TIME-DEPENDENT COMPRESSIBLE NAVIER-STOKES EQUATIONS AT HIGH REYNOLDS NUMBER

Robert W. MacCormack

Ames Research Center, NASA
Moffett Field, California, USA

ABSTRACT

This paper describes a new numerical method that has been used to drastically reduce the computation time required to solve the Navier-Stokes equations at flight Reynolds numbers. Though flows past complete aircraft configurations are still beyond our reach, the new method makes it possible and practical to calculate many important three-dimensional, high Reynolds number flow fields on today's computers.

INTRODUCTION

The Navier-Stokes equations adequately describe aerodynamic flows at standard atmospheric temperatures and pressures. If we could efficiently solve these equations, there would be no need for experimental tests to design flight vehicles or other aerodynamic devices. Unfortunately, analytic or closed-form solutions to these equations exist for only a few simple flow problems. During the past decade, the computer has been used to generate many new solutions. However, with existing numerical methods and computer resources, these solutions have been restricted to low Reynolds number or two-dimensional flows. This paper describes a new numerical method that has been used to drastically reduce the computation time required to solve the Navier-Stokes equations at flight Reynolds numbers. Though flows past complete aircraft configurations are still beyond our reach, the new method makes it possible and practical to calculate many important three-dimensional, high Reynolds number flow fields on today's computers.

The unsteady Navier-Stokes equations are difficult to solve because at high Reynolds numbers the magnitude of the inertial forces described by the hyperbolic terms of the equations are much larger than the viscous forces described by the parabolic terms. Conventional numerical methods, whether explicit or implicit, are severely restricted to small time steps by the stability or accuracy requirements imposed by the hyperbolic terms; hence, many time steps may be required before the viscous effects can be determined. The present approach time-splits the equations into a hyperbolic part and a parabolic part, solves the hyperbolic part by using a new explicit numerical method based on characterisitics theory, and solves the parabolic part by using

a new efficient implicit parabolic method. Both methods are fully conservative and stable with time-steps orders of magnitude larger than those allowed by CFL (Courant, Friedrich, and Lewy) stability criteria.

DIFFERENTIAL EQUATIONS

The time-dependent compressible Navier-Stokes equations in two dimensions may be written in conservation form as

$$\frac{\partial U}{\partial t} + \frac{\partial F}{\partial x} + \frac{\partial G}{\partial y} = 0 \qquad (1)$$

where $U = \begin{pmatrix} \rho \\ \rho u \\ \rho v \\ e \end{pmatrix}$, $F = \begin{pmatrix} \rho u \\ \rho u^2 + \sigma_x \\ \rho uv + \tau_{xy} \\ (e + \sigma_x)u + \tau_{yx}v - \kappa \frac{\partial \varepsilon}{\partial x} \end{pmatrix}$, $G = \begin{pmatrix} \rho v \\ \rho uv + \tau_{yx} \\ \rho v^2 + \sigma_y \\ (e + \sigma_y)v + \tau_{xy}u - \kappa \frac{\partial \varepsilon}{\partial y} \end{pmatrix}$

$$\sigma_x = p - \lambda\left(\frac{\partial u}{\partial x} + \frac{\partial v}{\partial y}\right) - 2\mu \frac{\partial u}{\partial x}, \quad \tau_{xy} = \tau_{yx} = -\mu\left(\frac{\partial u}{\partial y} + \frac{\partial v}{\partial x}\right)$$

and $$\sigma_y = p - \lambda\left(\frac{\partial u}{\partial x} + \frac{\partial v}{\partial y}\right) - 2\mu \frac{\partial v}{\partial y}$$

in terms of density ρ, x and y velocity components u and v, viscosity coefficients λ and μ, total energy per unit volume e, specific internal energy ε, and coefficient of heat conductivity κ. Finally, the pressure p is related to ε and ρ by an equation of state, $p(\varepsilon,\rho)$, where $\varepsilon = (e/\rho) - [(u^2 + v^2)/2]$.

COMPUTATIONAL MESH

For calculating inviscid-viscous interacting flows such as that sketched in Fig. 1 for a shock wave boundary-layer interaction, an efficient

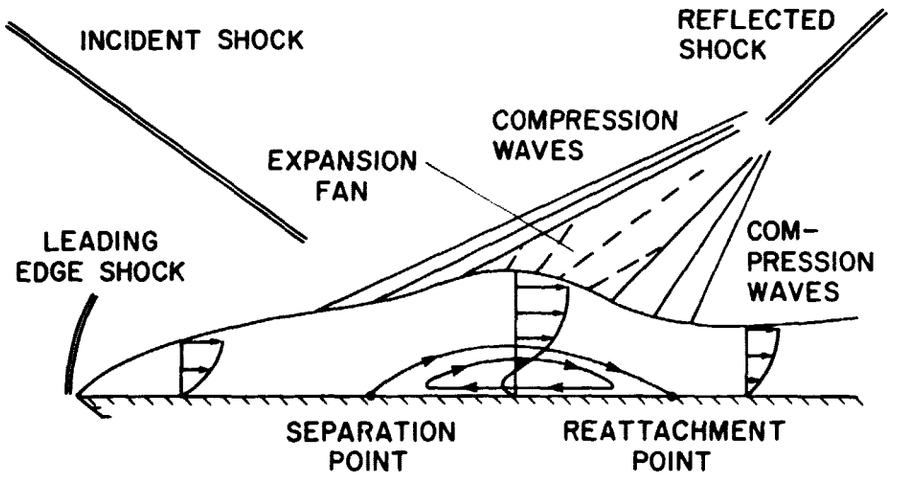

Fig. 1 Shock wave boundary-layer interaction

computational mesh is used, shown in Fig. 2. It consists of a fine mesh near the wall for resolving the flow where viscous effects are important and a coarse mesh away from the wall where the flow is essentially inviscid. Additional efficiency can be gained by stretching the fine mesh away from the wall to reduce the number of mesh points in regions requiring less resolution.

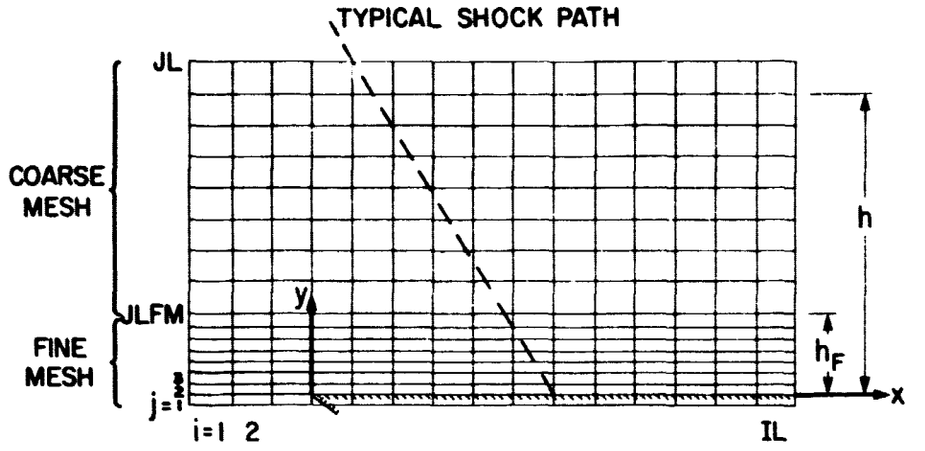

Fig. 2 Computational mesh for inviscid-viscous interaction flows

FORMER METHOD

In 1970 a second-order accurate numerical method was presented (1) for solving the unsteady compressible Navier-Stokes equations for inviscid-viscous interaction problems. Since then, the method to be called "former" in this paper, has been significantly modified (2) to increase its accuracy and efficiency. A brief description of it follows.

If the solution $U^n_{i,j}$ is known at time $t = n\Delta t$ at each mesh point (i,j), the solution at time $t = (n + 1)\Delta t$ is calculated by

$$U^{n+1}_{i,j} = \mathcal{L}(\Delta t)U^n_{i,j}$$

where $\mathcal{L}(\Delta t)$ is a symmetric sequence of time-split, one-dimensional difference operators $\mathcal{L}_x(\Delta t_x)$ and $\mathcal{L}_y(\Delta t_y)$. For example,

$$U^{n+1}_{i,j} = \mathcal{L}_x\left(\frac{\Delta t}{2}\right)\mathcal{L}_y(\Delta t)\mathcal{L}_x\left(\frac{\Delta t}{2}\right)U^n_{i,j}$$

In this sequence the $\mathcal{L}_x$ operator is called twice, each time advancing the solution in time by $\Delta t/2$ by accounting only for the effect of the x-derivative in Eq. (1) on the solution. Similarly, the $\mathcal{L}_y$ operator advances the solution by Δt once by accounting only for the effect of the y-derivative on the solution. The $\mathcal{L}_y$ operator solves the time-split differential "equation"

$$\frac{\partial U}{\partial t} + \frac{\partial G}{\partial y} = 0$$

by first predicting a new value $U^{(p)}_{i,j}$ from the current solution value $U_{i,j}$

$$U^{(p)}_{i,j} = U_{i,j} - \frac{\Delta t}{\Delta y}(G_{i,j} - G_{i,j-1})$$

and then correcting the predicted value,

$$U^{(c)}_{i,j} = \frac{1}{2}\left\{U_{i,j} + U^{(p)}_{i,j} - \frac{\Delta t}{\Delta y}\left[G^{(p)}_{i,j+1} - G^{(p)}_{i,j}\right]\right\}$$

The corrected value then becomes the current value for the next split difference operator in the sequence. The operator $\mathcal{L}_x$ is similarly defined.

The operators $\mathcal{L}_x(\Delta t_x)$ and $\mathcal{L}_y(\Delta t_y)$ are stable if

$$\Delta t_x \leq \frac{\Delta x}{|u| + c + (1/\rho)\{(2\gamma\mu/Pr\Delta x) + [(-\lambda\mu)^{1/2}/\Delta y]\}}$$

and

$$\Delta t_y \leq \frac{\Delta y}{|v| + c + (1/\rho)\{[(-\lambda\mu)^{1/2}/\Delta x] + (2\gamma\mu/Pr\Delta y)\}}$$

where c is the speed of sound, γ is the ratio of specific heats of the gas, and Pr is the Prandtl number.

For calculating an inviscid-viscous interacting flow on a two-mesh system shown in Fig. 2, typical operator sequences are (1) for all (i,j) in the coarse mesh

$$U^{n+1}_{i,j} = \mathcal{L}_x\left(\frac{\Delta t}{2}\right)\mathcal{L}_y(\Delta t)\mathcal{L}_x\left(\frac{\Delta t}{2}\right)U^n_{i,j}$$

where $\Delta t \leq \min_{i,j}\{2 \max \Delta t_x, \max \Delta t_y\}$, and (2) for all (i,j) in the fine mesh

$$U^{n+1}_{i,j} = \left[\mathcal{L}_y\left(\frac{\Delta t}{2m}\right)\mathcal{L}_x\left(\frac{\Delta t}{m}\right)\mathcal{L}_y\left(\frac{\Delta t}{2m}\right)\right]^m U^n_{i,j}$$

where m is the smallest integer such that $(\Delta t/m) \leq \min_{i,j}\{\max \Delta t_x, 2 \max \Delta t_y\}$.

For high Reynolds number calculations, the viscous region becomes very thin, requiring Δy near the wall to be very small. This causes Δt_y of the $\mathcal{L}_y$ operator also to be small and the integer m to be large. Values for m often exceed 100, requring a great amount of calculation time in the fine mesh.

PRESENT METHOD

Two new operators have been developed for replacing the $\mathcal{L}_y$ operator in the fine-mesh calculation

$$\mathcal{L}_y(\Delta t) \longleftarrow \mathcal{L}_{y_H}(\Delta t)\mathcal{L}_{y_P}(\Delta t)$$

The operator $\mathcal{L}_{y_H}$ solves for the inviscid (hyperbolic) terms of G. It is explicit, conservative, uses characteristic relations to predict convection and pressure fields, and is stable if

$$\Delta t \leq \frac{\Delta y}{|v|}$$

Because the fine mesh covers only a thin layer of the flow adjacent to the wall, the normal to the wall velocity component v is very small relative to c; hence, the above stability bound for $\mathcal{L}_{y_H}$ is much less restrictive than that for $\mathcal{L}_y$.

The operator $\mathcal{L}_{y_P}$ solves for the viscous (parabolic) terms of G. It is implicit, conservative, requires no linearization, uses simple tridiagonal inversion instead of block tridiagonal inversion procedures, and is unconditionally stable.

The operator sequence for all (i,j) in the fine mesh for the present method is

$$U^{nH}_{i,j} = \left[\mathcal{L}_{y_H}\left(\frac{\Delta t}{2m}\right)\mathcal{L}_{y_P}\left(\frac{\Delta t}{2m}\right)\mathcal{L}_x\left(\frac{\Delta t}{m}\right)\mathcal{L}_{y_P}\left(\frac{\Delta t}{2m}\right)\mathcal{L}_{y_H}\left(\frac{\Delta t}{2m}\right)\right]^m U^n_{i,j}$$

where now, because of the greatly relaxed stability requirements, m is a small integer usually equal to 2 in value.

THE OPERATOR $\mathcal{L}_{y_H}$

The operator $\mathcal{L}_{y_H}$ solves the split conservation law "equation"

$$\frac{\partial U}{\partial t} + \frac{\partial G_H}{\partial y} = 0 \quad \text{where} \quad G_H = \begin{pmatrix} \rho\underline{v} \\ \rho u\underline{v} \\ \rho v\underline{v} + \underline{p} \\ (e + \underline{p})\underline{v} \end{pmatrix} \tag{2}$$

The convection velocity v and pressure p have been underlined for later reference. Conventional explicit difference methods for this equation are limited to time steps

$$\Delta t \leq \frac{\Delta y}{|v| + c}$$

Violation of this condition, the CFL condition, is a violation of the domain of dependence principle and usually results in rapid numerical error growth. The operator $\mathcal{L}_{y_H}$ with time steps $\Delta t \leq (\Delta y/|v|)$ circumvents the CFL condition by first predicting at time $t + \Delta t$ the convection and pressure fields using characteristic relations which do not violate the domain of dependence principle and then by using the predicted values, values at time t, and the equations of motion to determine the time-averaged velocity and pressure gradients at each mesh point (i,j) to be used to integrate the above equation in a way similar to that described for the operator $\mathcal{L}_y$.

To derive the required characteristic relations, we first write the above equation in nonconservation form

$$\frac{\partial U'}{\partial t} + B\frac{\partial U'}{\partial y} = 0 \quad \text{where} \quad U' = \begin{pmatrix} \rho \\ u \\ v \\ p \end{pmatrix}$$

$$B = \begin{pmatrix} v & 0 & \rho & 0 \\ 0 & v & 0 & 0 \\ 0 & 0 & v & 1/\rho \\ 0 & 0 & \gamma p & v \end{pmatrix} = vI + \begin{pmatrix} 0 & 0 & \rho & 0 \\ 0 & 0 & 0 & 0 \\ 0 & 0 & 0 & 1/\rho \\ 0 & 0 & \gamma p & 0 \end{pmatrix}$$

If v is negligible compared to c, then the equations of motion become

$$\frac{\partial v}{\partial t} + \frac{1}{\rho}\frac{\partial p}{\partial y} = 0$$

and

$$\frac{\partial p}{\partial t} + \gamma p \frac{\partial v}{\partial y} = 0$$

Using the relation $c = \sqrt{\gamma \frac{p}{\rho}}$, we obtain the following characteristic relations

$$\frac{dp}{d\xi_+} + \rho c \frac{dv}{d\xi_+} = 0 \quad \text{where} \quad \frac{d}{d\xi_+} = \frac{\partial}{\partial t} + c\frac{\partial}{\partial y}$$

and

$$\frac{dp}{d\xi_-} - \rho c \frac{dv}{d\xi_-} = 0 \quad \text{where} \quad \frac{d}{d\xi_-} = \frac{\partial}{\partial t} - c\frac{\partial}{\partial y}$$

These relations can be solved rapidly for large time steps on a characteristic set of mesh points such as that shown in Fig. 3. The characteristic mesh

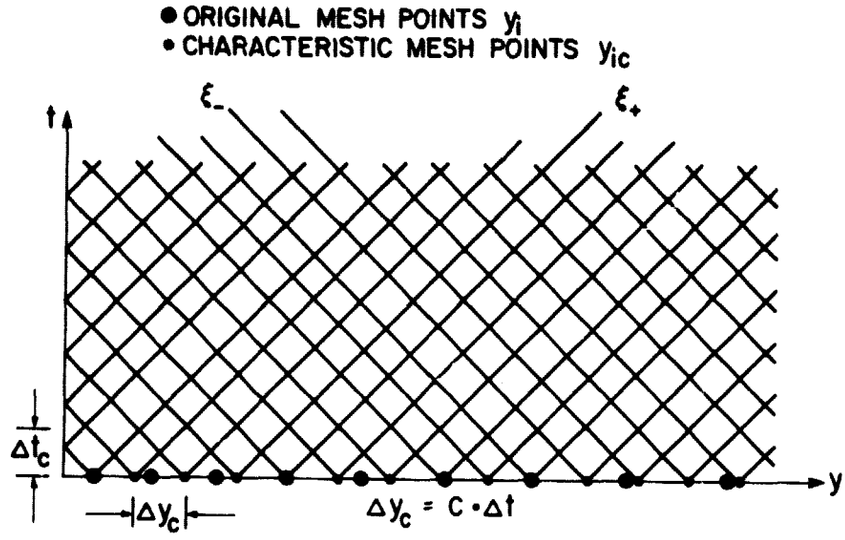

Fig. 3 Characteristic mesh

points $\{y_{jc}, jc = 1,2,3 \ldots\}$ are spaced according to the local speed of sound, although they are shown equally spaced in the figure. The first characteristic mesh point is positioned $c_w \Delta t_c/2$ away from the wall, where c_w is the speed of sound at the wall and $\Delta t_c = \min_{i,j}(\Delta y/c)$. The $jc + 1^{st}$ mesh point is given by $y_{jc+1} = y_{jc} + c_{jc}\Delta t_c$ where c_{jc} is found by interpolation from values at the original set of mesh points $\{y_j, j = 1,2 \ldots\}$. The dependent variables ρ_{jc}, v_{jc}, and p_{jc} are also obtained at each of the new mesh points by interpolation. The new mesh has the following property: a sound signal traveling either to the right or left can leave any point in the mesh at time t and arrive at its next neighbor at $t + \Delta t_c$, and at its next neighbor at $t + 2\Delta t_c$, etc. This property can be used to solve quickly for v and p at time $t^* = t + k\Delta t_c$, as shown in Fig. 4, where k is the largest integer such that $k\Delta t_c \le \min_{i,j}(\Delta y/|v|)$. Approximating the characteristic relations by

$$p^*_{jc} - p_{jc-k} + \rho_{jc} c_{jc}(v^*_{jc} - v_{jc-k}) = 0$$

and

$$p^*_{jc} - p_{jc+k} - \rho_{jc} c_{jc}(v_{jc} - v_{jc+k}) = 0$$

we obtain

$$p^*_{jc} = \frac{p_{jc-k} + p_{jc+k}}{2} + \rho_{jc} c_{jc} \frac{v_{jc-k} - v_{jc+k}}{2}$$

$$v^*_{jc} = \frac{v_{jc-k} + v_{jc+k}}{2} + \frac{p_{jc-k} - p_{jc+k}}{2\rho_{jc} c_{jc}}$$

For characteristic paths reflecting from the wall, $jc - k \le 0$, and p_{jc-k} and v_{jc-k} are replaced by $p_{1-(jc-k)}$ and $-v_{1-(jc-k)}$, respectively.

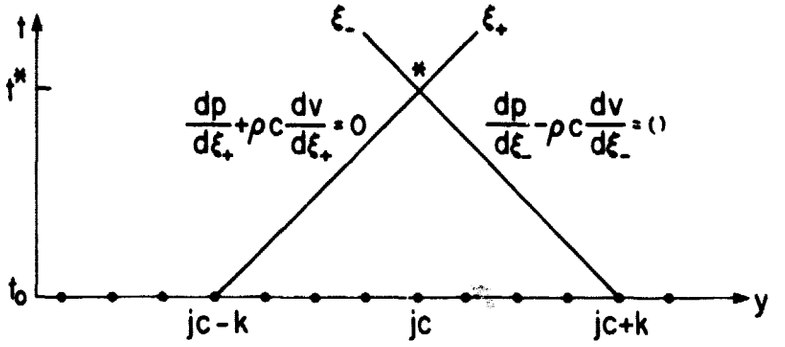

Fig. 4 Characteristic solution

An alternative solution technique and the one used by the present method is to replace the point values by integrated space-averaged values. Thus,

$$p^*_{jc} = \frac{P_{-jc} + P_{+jc}}{2} + \rho_{jc} c_{jc} \frac{V_{-jc} - V_{+jc}}{2}$$

and

$$v^*_{jc} = \frac{V_{-jc} + V_{+jc}}{2} + \frac{P_{-jc} - P_{+jc}}{2\rho_{jc} c_{jc}}$$

where

$$P_{-jc} = \frac{1}{2k+1} \sum_{\ell=0}^{2k} p_{jc-\ell}\ , \quad P_{+jc} = \frac{1}{2k+1} \sum_{\ell=0}^{2k} p_{jc+\ell}\ ,$$

$$V_{-jc} = \frac{1}{2k+1} \sum_{\ell=0}^{2k} v_{jc-\ell}\ , \text{ and } V_{+jc} = \frac{1}{2k+1} \sum_{\ell=0}^{2k} v_{jc+\ell}$$

Once the integrated averages have been determined for point jc, only four additions and four subtractions are required to obtain the values for point $jc + 1$ for any k.

Using the values of v and p at times t and t^* and the equations of motion, we can determined the time-averaged velocity and pressure gradients responsible for the change in the solution

$$\overline{\frac{\partial v}{\partial y_{jc}}} = \frac{1}{\Delta t} \int_t^{t^*} \frac{\partial v}{\partial y_{jc}}\, dt$$

$$= \frac{1}{\Delta t} \int_t^{t^*} -\frac{1}{\gamma p} \frac{\partial p}{\partial t_{jc}}\, dt = -\frac{p^*_{jc} - p_{jc}}{\rho_{jc} c^2_{jc} \Delta t}$$

and

$$\overline{\frac{\partial p}{\partial y_{jc}}} = \frac{1}{\Delta t} \int_t^{t^*} \frac{\partial p}{\partial y_{jc}}\, dt$$

$$= \frac{1}{\Delta t} \int_t^{t^*} -\rho \frac{\partial v}{\partial t_{jc}}\, dt = -\rho_{jc} \frac{v^*_{jc} - v_{jc}}{\Delta t}$$

where $\Delta t = k\Delta t_c = t - t^*$.

These are the velocity and pressure gradients which will be used to integrate Eq. (2). We first numerically integrate the gradients in y to determine v and p at each of the original set of mesh points $\{y_j, j = 1,2,3 \ldots\}$

$$\bar{v}_j = \int_0^{y_j} \frac{\overline{\partial v}}{\partial y_{jc}} \, dy_{jc}$$

and

$$\bar{p}_j = p_w + \int_0^{y_j} \frac{\partial p}{\partial y_{jc}} \, dy_{jc}$$

where p_w is pressure at the wall and is found by a characteristic relation similar to the ones given earlier. Equation (2) can now be integrated in time by $\Delta t = k\Delta t_c$ in the fine mesh in the same manner as described for the former method except that the convection velocity and pressure (the underlined terms of G_H) are replaced by their time-averaged values determined above in both the predictor and corrector steps.

THE OPERATOR $\mathcal{L}_{y_p}$

The operator $\mathcal{L}_{y_p}$ solves the split conservation law "equation"

$$\frac{\partial U}{\partial t} + \frac{\partial G_P}{\partial y} = 0 \quad \text{where} \quad G_P = G - G_H \tag{3}$$

This equation is parabolic and from domain of dependence considerations it is most appropriately solved using an implicit numerical method. Examples of such methods applied to the following model parabolic equation

$$\frac{\partial u}{\partial t} = \frac{\partial \mu(\partial u/\partial y)}{\partial y} + [\text{small terms}]$$

are (a) Crank-Nicolson

$$u_j^{n+1} = u_j^n + \frac{\mu\Delta t}{2\Delta y^2}\left(u_{j-1}^n - 2u_j^n + u_{j+1}^n\right) + \frac{\mu\Delta t}{2\Delta y^2}\left(u_{j-1}^{n+1} - 2u_j^{n+1} + u_{j+1}^{n+1}\right) + \Delta t\,[\text{small terms}]$$

and (b) Laasonen

$$u_j^{n+1} = u_j^n + \frac{\mu\Delta t}{\Delta y^2}\left(u_{j-1}^{n+1} - 2u_j^{n+1} + u_{j+1}^{n+1}\right) + \Delta t\,[\text{small terms}]$$

The above difference equations can be efficiently solved by a simple tridiagonal inversion.

Equation (3) can be written

$$\frac{\partial \rho}{\partial t} = 0$$

$$\frac{\partial u}{\partial t} = \frac{1}{\rho}\frac{\partial[\mu(\partial u/\partial y)]}{\partial y} + \frac{1}{\rho}\left\{\frac{\partial[\mu(\partial v/\partial x)]}{\partial y}\right\}$$

$$\frac{\partial v}{\partial t} = \frac{1}{\rho}\frac{\partial[(\lambda + 2\mu)(\partial v/\partial y)]}{\partial y} + \left\{\frac{1}{\rho}\frac{\partial[\lambda(\partial u/\partial x)]}{\partial y}\right\}$$

$$\frac{\partial\{\varepsilon + [(u^2 + v^2)/2]\}}{\partial t} = \frac{1}{\rho}\frac{\partial[\mu u(\partial u/\partial y) + (\lambda + 2\mu)v(\partial v/\partial y) + k(\partial\varepsilon/\partial y)]}{2y}$$

$$+ \left\{\frac{1}{\rho}\frac{\partial[\mu u(\partial v/\partial w) + \lambda(\partial u/\partial x)]}{\partial y}\right\}$$

The first of the above equations, the continuity equation without convection, indicates that density is stationary in time during this time-split interval and is thus trivially solved. The second and third equations, the x and y momentum equations, have essentially the same form as the model parabolic equation and can be efficiently solved using two simple tridiagonal inversions. Unfortunately, the fourth equation, the total energy equation, does not have the same form as the model equation because the solution variable $\varepsilon + [(u^2 + v^2)/2]$ does not appear on the right-hand side in a second derivative with respect to the y term, although parts of it do. To avoid using a more costly block tridiagonal procedure for solution, we split the energy equation into three equations, a u^2 kinetic energy equation, a v^2 kinetic energy equation, and an internal energy equation. We obtain the kinetic energy equations by multiplying the x and y momentum equations by u and v, respectively. The internal energy equation is obtained by subtracting the two kinetic energy equations from the total energy equation. The resulting equations in model parabolic form are

$$\frac{\partial u^2}{\partial t} = \frac{1}{\rho}\frac{\partial[\mu(\partial u^2/\partial y)]}{\partial y} + \left\{\frac{1}{\rho}\frac{\partial[2\mu u(\partial v/\partial x)]}{\partial y} - T_1\right\}$$

$$\frac{\partial v^2}{\partial t} = \frac{1}{\rho}\frac{\partial[(\lambda + 2\mu)(\partial v^2/\partial y)]}{\partial y} + \left\{\frac{1}{\rho}\frac{\partial[(2\lambda v(\partial u/\partial x)]}{\partial y} - T_2\right\}$$

$$\frac{\partial\varepsilon}{\partial t} = \frac{1}{\rho}\frac{\partial[k(\partial\varepsilon/\partial y)]}{\partial y} + \left\{\frac{T_1 + T_2}{2}\right\}$$

where

$$T_1 = \frac{2}{\rho}\frac{\partial u}{\partial y}\left[\mu\left(\frac{\partial u}{\partial y} + \frac{\partial v}{\partial x}\right)\right]$$

and

$$T_2 = \frac{2}{\rho}\frac{\partial v}{\partial y}\left[(\lambda + 2\mu)\frac{\partial v}{\partial y} + \lambda\frac{\partial u}{\partial x}\right]$$

The u^2 and v^2 kinetic energy equations form the same tridiagonal coefficient matrices as the u and v momentum equations; hence, solution of the three energy equations requires the inversion of only one additional tridiagonal matrix.

The operator $\mathcal{L}_{y_p}$ solves Eq. (3) using either the Crank-Nicolson or the Lasonen method. The second-order accurate Crank-Nicolson method is preferred unless the coefficient $\mu\Delta t/\Delta y^2$ is large enough that the numerical amplification factor of the method approaches -1, at which point the Crank-Nicolson method is known to behave erratically. For large values of $\mu\Delta t/\Delta y^2$, the first-order accurate Lasonen method is used. The variations of ρ, μ, and λ in y cause no difficulty for either method. The variations of μ, λ, and the [small terms] on the right can be accounted for by solving the equations twice, first with the present values of μ, λ, and [small terms] and then with the newly calculated values. Averaging the two solutions time-centers the difference equations. The assumption that the mixed derivative terms can be treated as small terms has caused no numerical difficulties. The present method first solves the x and y momentum equations, uses the present and new u and v solutions to evaluate the dissipation terms T_1 and T_2 (not always small) in

either a Crank-Nicolson or Lassonen manner, and then solves the u^2, v^2, and ε energy equations. Errors made in the u^2, v^2, and ε equations because of large T_1 and T_2 cancel exactly when the solutions are combined to obtain $e = \rho\{\varepsilon + [(u^2 + v^2)/2]\}$.

The operator $\mathcal{L}_{y_p}$ inverts three simple tridiagonal coefficient matrices and solves five systems of equations. Using the convention of counting only multiplications and divisions (3), the present method requires 21N - 16 arithmetic operations, where N is the order of the tridiagonal system. Conventional methods for solving Eq. (3) invert one block tridiagonal matrix of order N with block element matrices of order three and require 108N - 18 operations if the inverses of the diagonal block element matrices are computed, or approximately 45N operations if the inverses are not computed.

RESULTS

Several shock wave boundary-layer interaction problems were calculated using the former method (2) and the present method. For each calculation the flow was at Mach 2, and a shock wave incident upon a flat plate increased the pressure by a factor of 1.4. Molecular viscosity was calculated using Sutherland's formula, and turbulent eddy viscosity was calculated using a Cebeci-Smith turbulence model. Figure 5 compares the results of both methods, experiment (4), and boundary-layer theory (Ref. 5, using Crocco's method) for a separated laminar boundary layer at a Reynolds number of 2.96×10^5. The results of the two methods agree well everywhere with the exception of pressure at the leading edge [Fig. 5(a)] which will be discussed herein. The present method required 1.0 min of CDC 7600 computer time, and the former method required 6.4 min. Figure 6 compares the results of both methods for a turbulent boundary-layer interaction at a Reynolds number of 2.96×10^6. Again the results of the two methods agree well except at the leading edge. Figure 6(c) displays the pressure profiles at the leading edge predicted by both methods. The present method is far more sensitive to the presence of the leading edge singularity than the former method and appears to be correctly approaching the theoretical value of pressure behind a Mach 2 normal shock wave. The present method required 1.4 min of computation time, and the former method required 58.5 min. Figure 7 compares the computing times of the former and present methods for a wide range of Reynolds numbers.

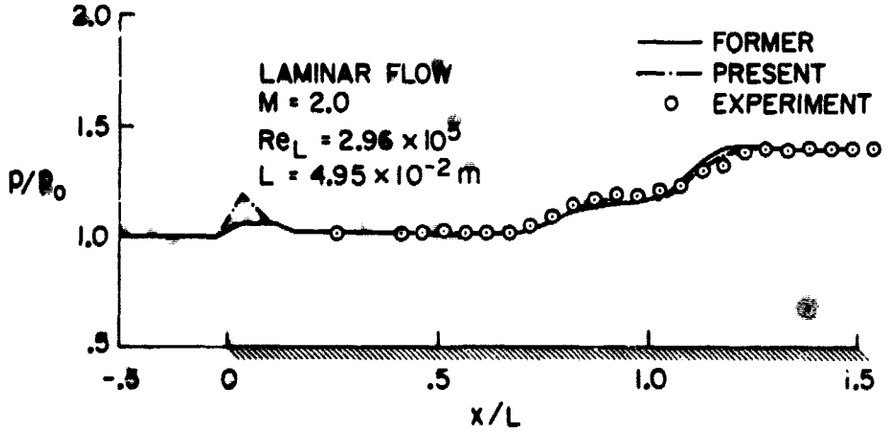

(a) Surface pressure

Fig. 5 Comparison of former and present method results for calculating laminar separated flow

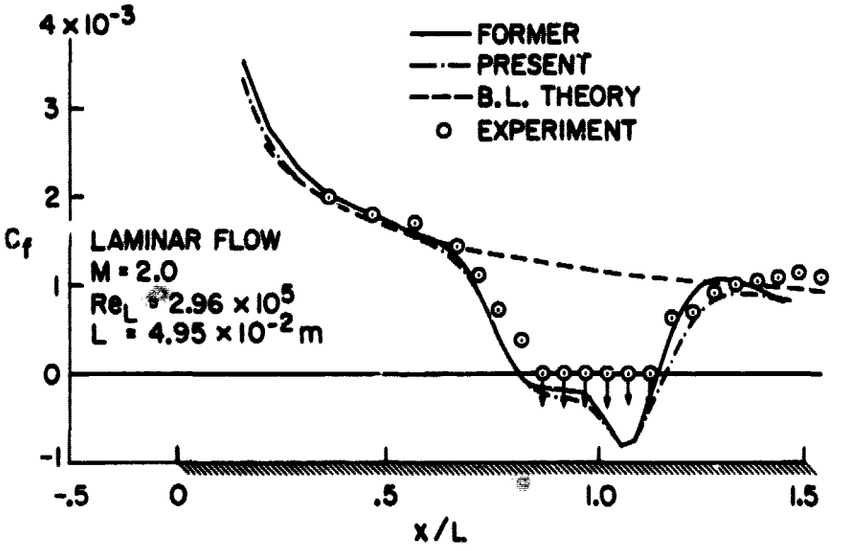

(b) Skin friction

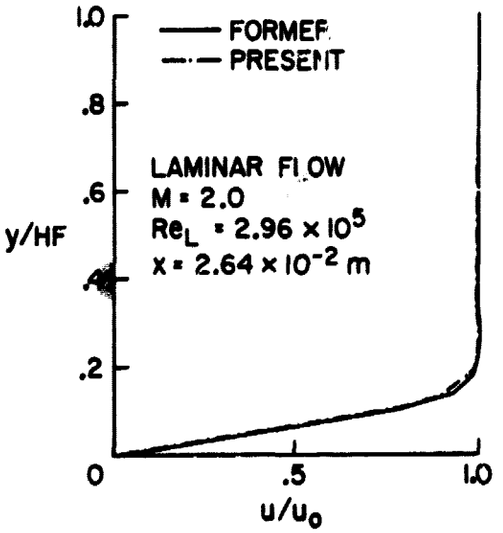

(c) Velocity profile ahead of separation

Fig. 5 Continued

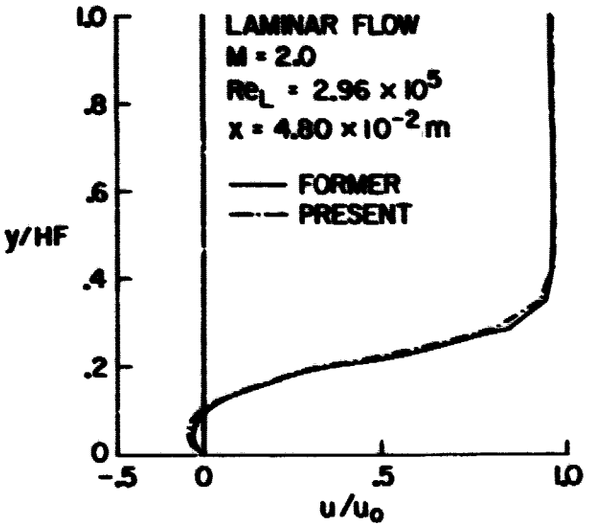

(d) Velocity profile interaction region

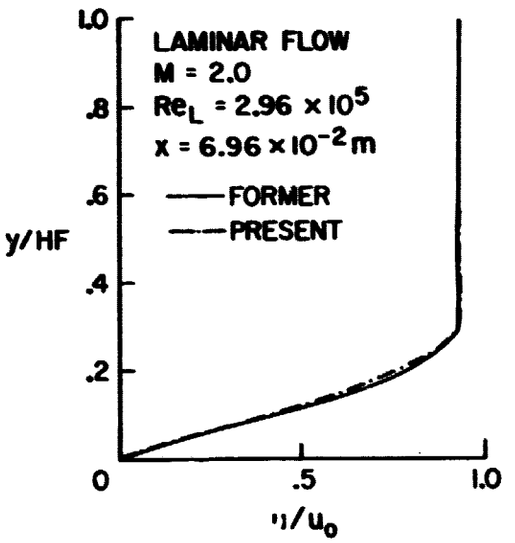

(e) Velocity profile aft of reattachment

Fig. 5 Concluded

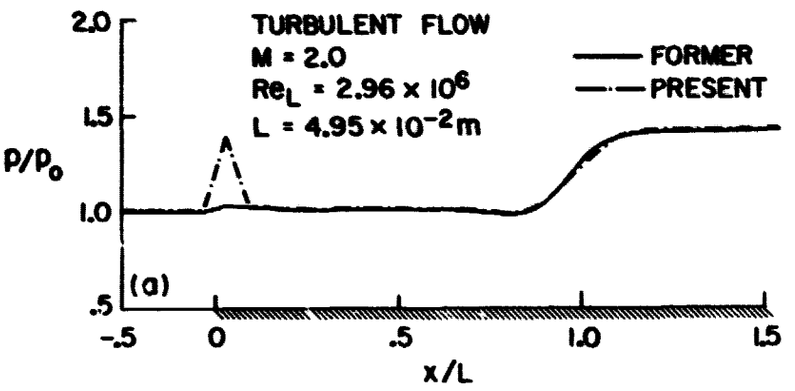

(a) Surface pressure

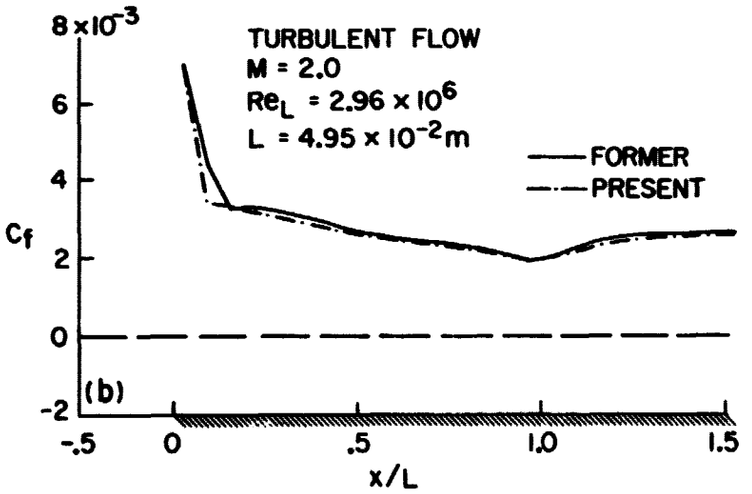

(b) Skin friction

Fig. 6 Comparison of former and present method results for calculating turbulent flow

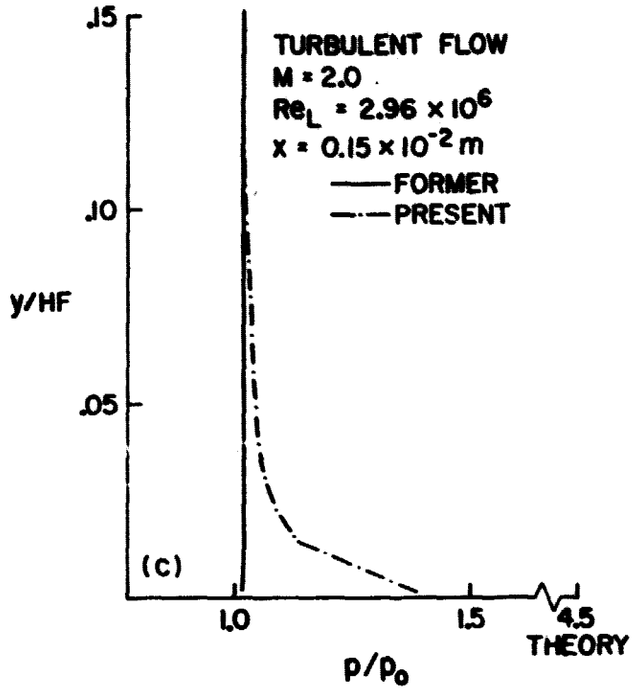

(c) Leading-edge singularity

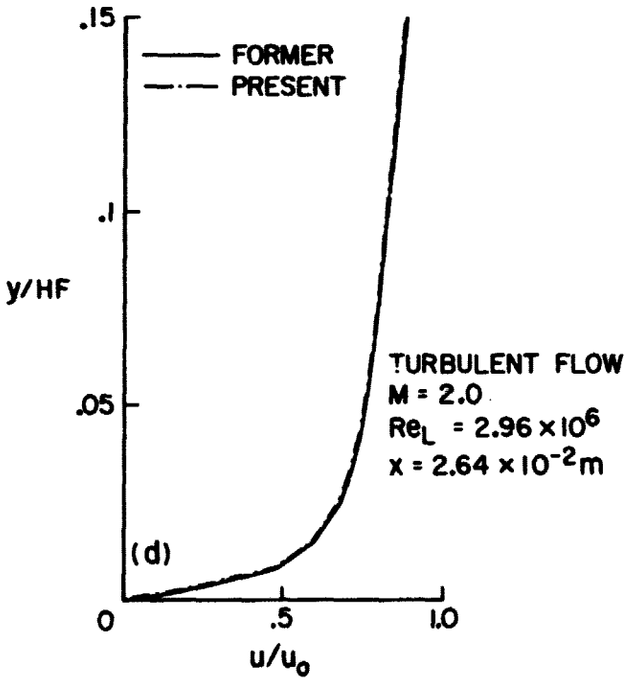

(d) Velocity profile ahead of interaction

Fig. 6 Continued

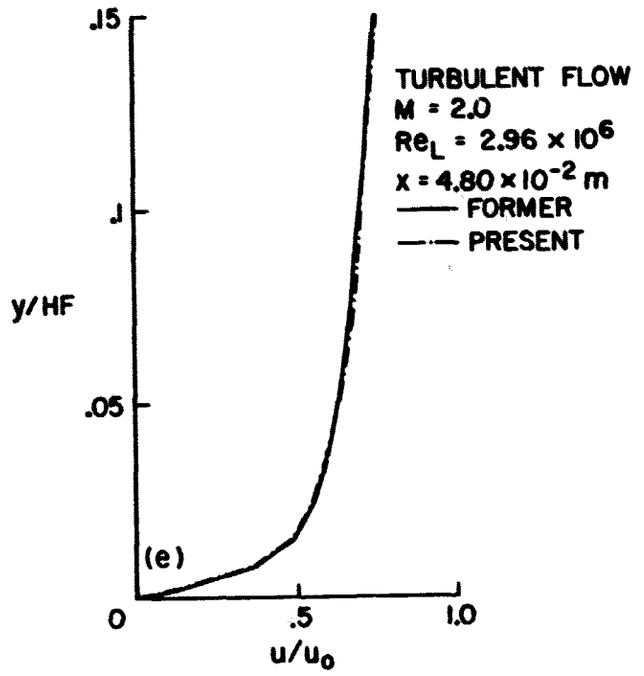

(e) Velocity profile interaction region

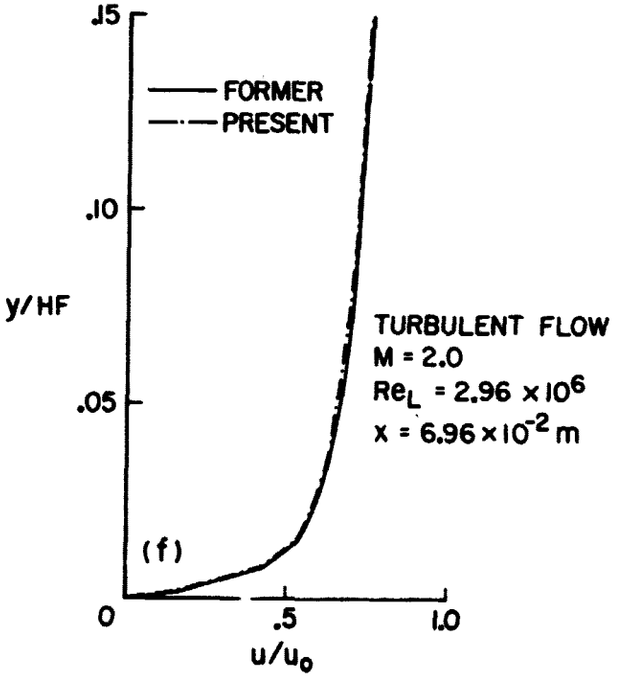

(f) Velocity profile aft of interaction

Fig. 6 Concluded

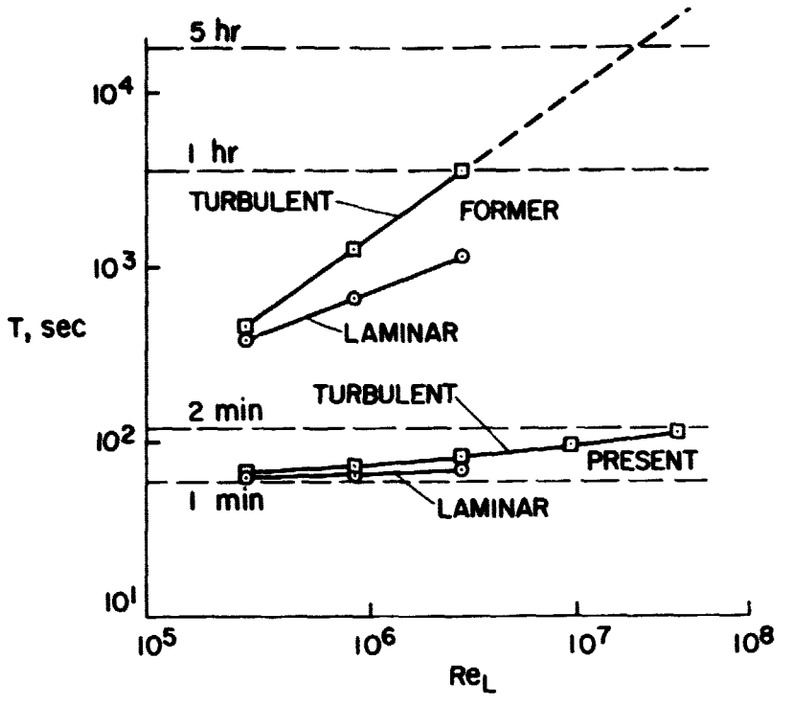

Fig. 7 Comparison of former and present method computing times on the CDC 7600 vs. Reynolds number for several shock boundary-layer interaction calculations

CONCLUSION

The present method has reduced the computation time by one and two orders of magnitude from that required previously to solve for the interaction of a shock wave with a boundary layer on a flat plate. The method has been applied with similar success to several other inviscid-viscous interaction problems, including flows past compression corners, wavy walls, axisymmetric channels, and blunt-nosed lifting airfoils, at Mach numbers as high as 8.5, with shock waves strong enough to increase surface pressure by a factor of 80, and at Reynolds numbers as high as 10^9.

REFERENCES

1. MacCormack, R. W., "Numerical Solution of the Interaction of a Shock Wave with a Laminar Boundary Layer," *Lecture Notes in Physics*, Vol. 8, Springer-Verlag, New York, 1971, p. 151.

2. MacCormack, R. W. and Baldwin, B. S., "A Numerical Method for Solving the Navier-Stokes Equations with Application to Shock Boundary Layer Interactions," AIAA Paper 75-1, presented at the AIAA 13th Aerospace Sciences Meeting, Pasadena, Calif., Jan. 20-22, 1975.

3. Isaacson, E. and Keller, H. B., *Analysis of Numerical Methods*, Wiley, New York, 1966.

4. Hakkinen, R. J., Greber, I., Trilling, L., and Abarbanel, S. S., "The Interaction of an Oblique Shock Wave with a Laminar Boundary Layer, NASA Memo 2-18-59W, 1959.

5. Van Driest, E. R., "Investigation of Laminar Boundary Layer in Compressible Fluids Using the Crocco Method," NASA TN-2597, 1952.